

PREPARED FOR SUBMISSION TO JHEP

## Effects of a Single Universal Extra Dimension in $B_c \rightarrow (D_s, D) \ell^+ \ell^-$ Decays

---

**Elif Danapinar and Umit Oktay Yilmaz**

*Physics Department, Karabuk University, Karabuk, Turkey*

*E-mail:* [elifdanapinar@gmail.com](mailto:elifdanapinar@gmail.com), [uoyilmaz@karabuk.edu.tr](mailto:uoyilmaz@karabuk.edu.tr)

**ABSTRACT:** The rare semileptonic  $B_c \rightarrow D_{s,d} \ell^+ \ell^-$  decays are studied in the universal extra dimension with a single extra dimension scenario. The sensitivity of differential and total branching ratios, polarization asymmetries of final state leptons to the compactification parameter is presented, both for muon and tau decay channels. Comparing with the standard model, the obtained results indicate that there are new contributions to the physical observables. Considering the ability of available experiments, it would be useful to study these effects.

**KEYWORDS:** extra dimension, semileptonic rare decay, lepton polarization

---

## Contents

<b>1</b>	<b>Introduction</b>	<b>1</b>
<b>2</b>	<b>Theoretical Framework</b>	<b>2</b>
<b>3</b>	<b>Matrix Elements and Decay Rate</b>	<b>3</b>
<b>4</b>	<b>Lepton Polarization Asymmetries</b>	<b>5</b>
<b>5</b>	<b>Numerical Analysis and Discussion</b>	<b>8</b>

---

## 1 Introduction

The decays induced by flavor changing neutral current (FCNC)  $b \rightarrow s, d$  transitions play an important role to test the standard model (SM) and also they are very sensitive to the new physics. The decays of  $B_{u,d,s}$  mesons have been intensively studied, and it will make the B physics more complete if similar decays of  $B_c$  meson are included. Considering the experimental facilities, it is possible to investigate  $B_c$  decays with present ability of the LHC.

In the rare  $B$  meson decays, new physics contributions appear through the modification of the Wilson coefficients existing in the SM or by adding new structures in the SM effective Hamiltonian. Among the various extensions of the SM, extra dimensions are specially attractive because of including gravity and other interactions, giving hints on the hierarchy problem and a connection with string theory.

The models with universal extra dimensions (UED) allow the SM fields to propagate in all available dimensions [1–4]. The extra dimensions are compactified and the compactification scale allows Kaluza-Klein (KK) partners of the SM fields in the four-dimensional theory and also KK excitations without corresponding SM partners. Throughout the UED, a model including only a single universal extra dimension is the Appelquist-Cheng-Dobrescu (ACD) model [5]. The only additional free parameter with respect to the SM is the inverse of the compactification radius,  $1/R$ . In particle spectrum of the ACD model, there are infinite towers of KK modes and the ordinary SM particles are presented in the zero mode.

Discussion on the free parameter, both experimental and theoretical aspects of the subject, shows that the lower bound should be between  $1/R \geq 250 \text{ GeV}$  or  $1/R \geq 350 \text{ GeV}$  [6–11]. Therefore, we will pay more attention to  $1/R = 250 - 350 \text{ GeV}$  region but also consider  $1/R = 200 - 1000 \text{ GeV}$  in our calculations.

The effective Hamiltonian of several FCNC processes [12]–[13], semileptonic and radiative decays of B mesons [14–22] and FCNC baryonic decays [10, 23–25] have been investigated in the ACD model. Polarization properties of final state particles in semileptonic

decays, which is an powerful tool in searching new physics beyond the SM, have also been studied widely besides the other observables in these works, e.g [11, 14, 18, 22].

The main aim of this paper is to find the possible effects of the ACD model on some physical observables related to the  $B_c \rightarrow (D_s, D)\ell^+\ell^-$  decays. We study differential decay rate, branching ratio, and polarization of final state leptons, including resonance contributions in as many as possible cases. We analyze these observables in terms of the compactification factor and the form factors. The form factors for  $B_c \rightarrow (D_s, D)\ell^+\ell^-$  processes have been calculated using different quark models [26–29] and three-point QCD sum rules [30]. In this work, we will use the form factors calculated in the constituent quark model [26].

This paper is organized as follows. In section 2, we give the effective Hamiltonian for the quark level processes  $b \rightarrow s, d \ell^+\ell^-$  with a brief discussion on the Wilson coefficients in the ACD model. We drive matrix element using the form factors and calculate the decay rate in section 3. In section 4, lepton polarizations are evaluated and in the last section, we introduce our numerical analysis and discuss the obtained results.

## 2 Theoretical Framework

The effective Hamiltonian describing the quark level  $b \rightarrow (s, d) \ell^+\ell^-$  processes in the SM is given by [31]

$$\begin{aligned} \mathcal{H}_{eff} = & \frac{G_F \alpha}{\sqrt{2}\pi} V_{tq'} V_{tb}^* \left[ C_9^{eff} (\bar{q}' \gamma_\mu L b) \bar{\ell} \gamma^\mu \ell + C_{10} (\bar{q}' \gamma_\mu L b) \bar{\ell} \gamma^\mu \gamma_5 \ell \right. \\ & \left. - 2C_7^{eff} m_b (\bar{q}' i \sigma_{\mu\nu} \frac{q^\nu}{q^2} R b) \bar{\ell} \gamma^\mu \ell \right], \end{aligned} \quad (2.1)$$

where  $q = p_{B_c} - p_{D_{q'}}$  is the momentum transfer and  $q' = s, d$ .

New physics effects in the ACD model come out by the modification of the SM Wilson coefficients appear in the above Hamiltonian. This process can be done by writing the Wilson coefficients in terms of  $1/R$  dependent periodic functions the details of which can be found in [12, 13]. That is,  $F_0(x_t)$  in the SM is generalized by  $F(x_t, 1/R)$  accordingly

$$F(x_t, 1/R) = F_0(x_t) + \sum_{n=1}^{\infty} F_n(x_t, x_n) \quad (2.2)$$

where  $x_t = m_t^2/m_W^2$ ,  $x_n = m_n^2/m_W^2$  and  $m_n = n/R$ . These modified Wilson coefficients can widely be found in the literature. Here, we will not discuss the details and follow the explanation given in [11].

In the ACD model, a normalization scheme independent effective coefficient  $C_7^{eff}$  can be written as

$$\begin{aligned} C_7^{eff}(\mu_b, 1/R) = & \eta^{16/23} C_7(\mu_W, 1/R) \\ & + \frac{8}{3} (\eta^{14/23} - \eta^{16/23}) C_8(\mu_W, 1/R) + C_2(\mu_W, 1/R) \sum_{i=1}^8 h_i \eta^{a_i}. \end{aligned} \quad (2.3)$$

The coefficient  $C_9^{eff}$  has perturbative part and we will also consider the resonance contributions coming from the conversion of the real  $c\bar{c}$  into lepton pair. So,  $C_9^{eff}$  is given by

$$C_9^{eff}(s', 1/R) = C_9(\mu, 1/R) \left( 1 + \frac{\alpha_s(\mu)}{\pi} w(s') \right) + Y(\mu) + C_9^{res}(\mu). \quad (2.4)$$

For  $C_9$ , in the ACD model and in the naive dimensional regularization (NDR) scheme we have

$$C_9(\mu, 1/R) = P_0^{NDR} + \frac{Y(x_t, 1/R)}{\sin^2 \theta_W} - 4Z(x_t, 1/R) + P_E E(x_t, 1/R) \quad (2.5)$$

where  $P_0^{NDR} = 2.60 \pm 0.25$  and the last term,  $P_E E(x_t, 1/R)$ , is numerically negligible. The perturbative part, coming from one-loop matrix elements of the four quark operators, is

$$\begin{aligned} Y(\mu) = & h(y, s) [3C_1(\mu) + C_2(\mu) + 3C_3(\mu) + C_4(\mu) + 3C_5(\mu) + C_6(\mu)] \\ & - \frac{1}{2} h(1, s) (4C_3(\mu) + 4C_4(\mu) + 3C_5(\mu) + C_6(\mu)) \\ & - \frac{1}{2} h(0, s) [C_3(\mu) + 3C_4(\mu)] \\ & + \frac{2}{9} (3C_3(\mu) + C_4(\mu) + 3C_5(\mu) + C_6(\mu)), \end{aligned} \quad (2.6)$$

with  $y = m_c/m_b$ . The explicit forms of the functions appear above equations can be found in [32, 33]. The resonance contribution can be done by using a Breit-Wigner formula [34]

$$\begin{aligned} C_9^{res} = & -\frac{3}{\alpha_{em}^2} \kappa \sum_{V_i=\psi_i} \frac{\pi \Gamma(V_i \rightarrow \ell^+ \ell^-) m_{V_i}}{s - m_{V_i}^2 + i m_{V_i} \Gamma_{V_i}} \\ & \times [3C_1(\mu) + C_2(\mu) + 3C_3(\mu) + C_4(\mu) + 3C_5(\mu) + C_6(\mu)]. \end{aligned} \quad (2.7)$$

The normalization is fixed by the data in [35] and  $\kappa$  is taken 2.3.

The Wilson coefficient  $C_{10}$  is independent of scale  $\mu$  and given by

$$C_{10} = -\frac{Y(x_t, 1/R)}{\sin^2 \theta_W}. \quad (2.8)$$

### 3 Matrix Elements and Decay Rate

The matrix elements for  $B_c \rightarrow D_{q'} \ell^+ \ell^-$  can be written in terms of the invariant form factors over  $B_c$  and  $D_{q'}$ . The parts of transition currents containing  $\gamma_5$  do not contribute, so the non-vanishing matrix elements are [36]

$$\begin{aligned} \langle D_{q'}(p_{D_{q'}}) | \bar{q}' i \sigma_{\mu\nu} q^\nu b | B_c(p_{B_c}) \rangle &= -\frac{f_T(q^2)}{m_{B_c} + m_{D_{q'}}} \left[ (P_{B_c} + P_{D_{q'}})_\mu q^2 - q_\mu (m_{B_c}^2 - m_{D_{q'}}^2) \right], \\ \langle D_{q'}(p_{D_{q'}}) | \bar{q}' \gamma_\mu b | B_c(p_{B_c}) \rangle &= f_+(q^2) (P_{B_c} + P_{D_{q'}})_\mu + f_-(q^2) q_\mu. \end{aligned} \quad (3.1)$$

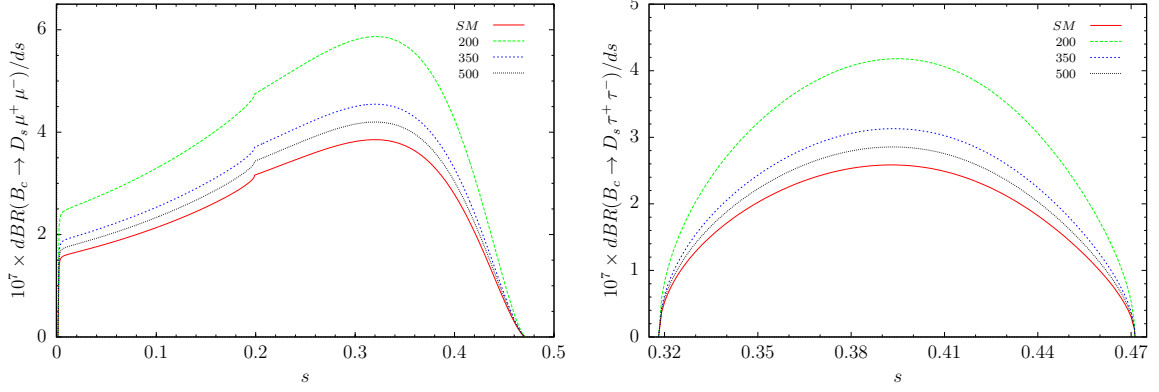


**Figure 1.** (color online) The dependence of differential branching ratio on  $s$  without resonance contributions for  $B_c \rightarrow D_s \ell^+ \ell^-$ . (In the legend  $1/R = 200, 350, 500 \text{ GeV}$ .)

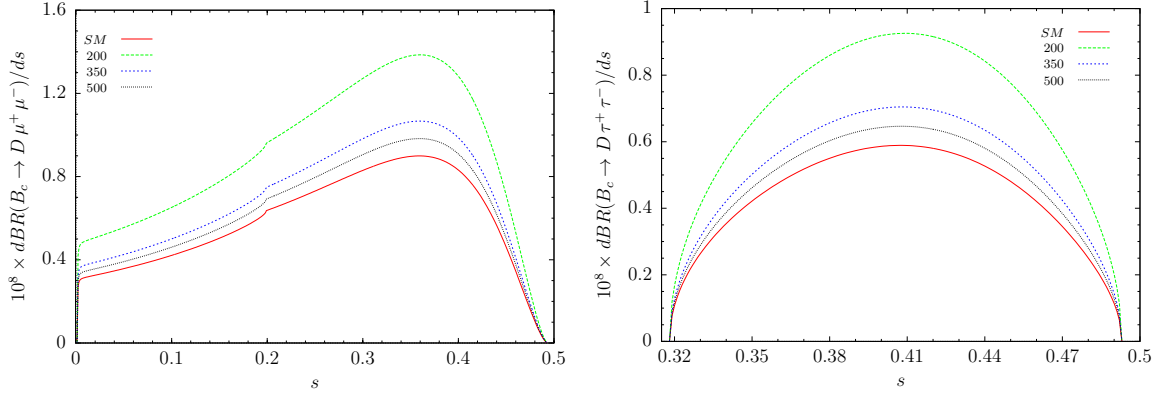


**Figure 2.** (color online) The dependence of differential branching ratio on  $s$  without resonance contributions for  $B_c \rightarrow D \ell^+ \ell^-$ .

The transition amplitude of the  $B_c \rightarrow D_{q'} \ell^+ \ell^-$  decays can be written using the effective Hamiltonian and eq. (3.1) as

$$\begin{aligned} \mathcal{M}(B_c \rightarrow D_{q'} \ell^+ \ell^-) = & \frac{G\alpha}{2\sqrt{2}\pi} V_{tb} V_{tq'}^* \left\{ \bar{\ell} \gamma^\mu \ell \left[ A(P_{B_c} + P_{D_{q'}})_\mu + B q_\mu \right] \right. \\ & \left. + \bar{\ell} \gamma^\mu \gamma_5 \ell \left[ C(P_{B_c} + P_{D_{q'}})_\mu + D q_\mu \right] \right\}, \end{aligned} \quad (3.2)$$

with

$$\begin{aligned} A &= C_9^{eff} f_+ + \frac{2m_b f_T}{m_{B_c} + m_{D_{q'}}} C_7^{eff}, \\ B &= C_9^{eff} f_- - \frac{2m_b(m_{B_c}^2 - m_{D_{q'}}^2) f_T}{q^2(m_{B_c} + m_{D_{q'}})} C_7^{eff}, \\ C &= C_{10} f_+, \\ D &= C_{10} f_-. \end{aligned} \quad (3.3)$$

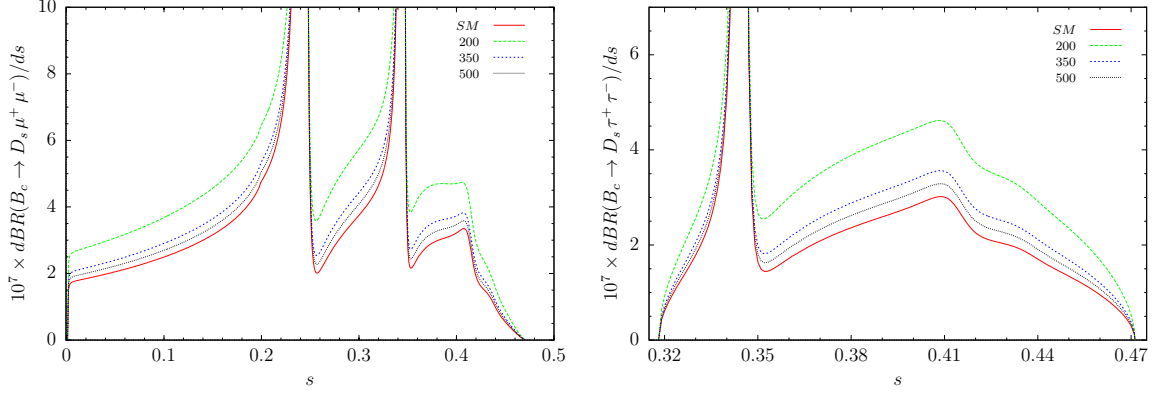


**Figure 3.** (color online) The dependence of differential branching ratio on  $s$  with resonance contributions for  $B_c \rightarrow D_s \ell^+ \ell^-$ .

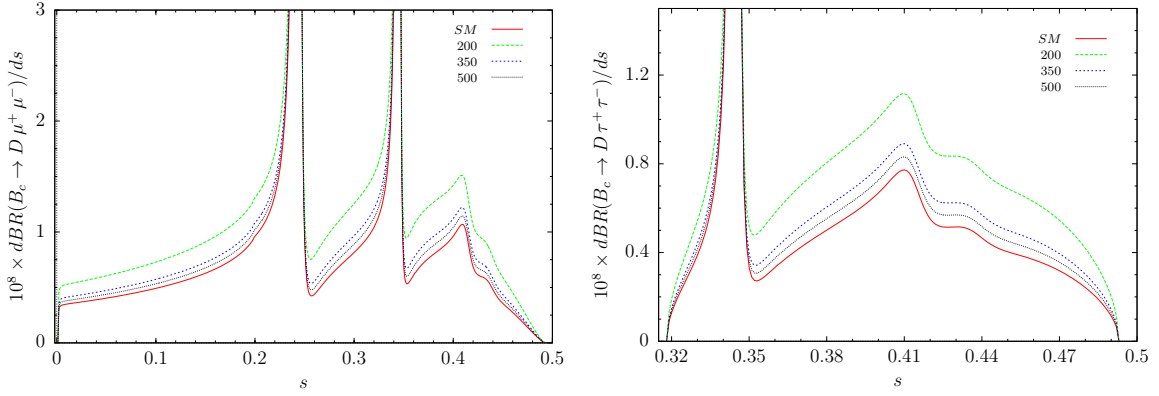


**Figure 4.** (color online) The dependence of differential branching ratio on  $s$  with resonance contributions for  $B_c \rightarrow D \ell^+ \ell^-$ .

Finally, following dilepton mass spectrum is obtained by eliminating angular dependence in the double differential decay rate,

$$\frac{d\Gamma}{ds} = \frac{G^2 \alpha^2 m_{B_c}}{2^{12} \pi^5} |V_{tb} V_{tq'}^*|^2 \sqrt{\lambda} v \Delta_{D_{q'}} \quad (3.4)$$

where  $s = q^2/m_{B_c}^2$ ,  $\lambda = 1 + r^2 + s^2 - 2r - 2s - 2rs$ ,  $r = m_{D_s^*}^2/m_{B_c}^2$ ,  $v = \sqrt{1 - 4m_\ell^2/sm_{B_c}^2}$  and

$$\begin{aligned} \Delta_{D_{q'}} = & \frac{4}{3} m_{B_c}^4 (3 - v^2) \lambda (|A|^2 + |C|^2) + 4 m_{B_c}^4 s (2 + r - s) (1 - v^2) |C|^2 \\ & + 16 m_{B_c}^2 m_\ell^2 s |D|^2 + 32 m_{B_c}^2 m_\ell^2 (1 - r) \text{Re}(CD^*). \end{aligned} \quad (3.5)$$

#### 4 Lepton Polarization Asymmetries

Studying polarization asymmetries of final state leptons is an useful way of searching new physics. Therefore, we will discuss the possible effects of the ACD model in the lepton

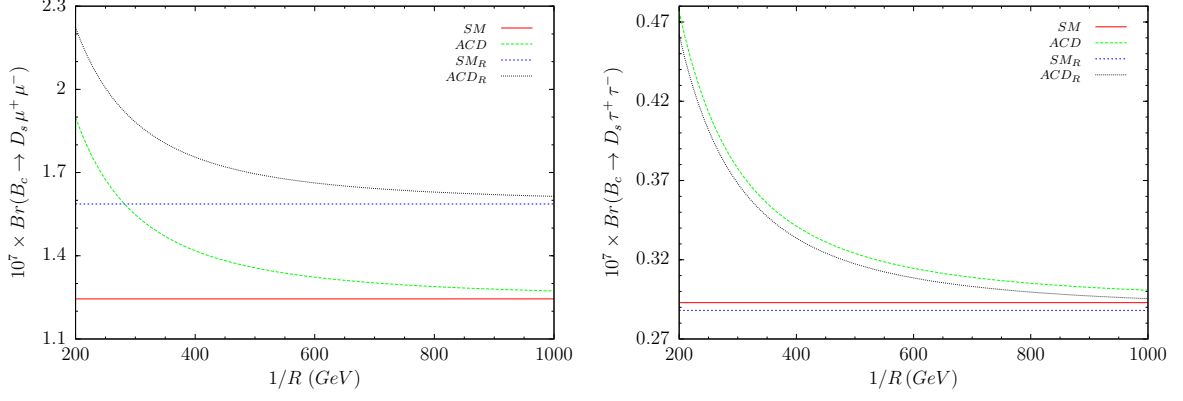


**Figure 5.** (color online) The dependence of branching ratio on  $1/R$  with and without resonance contributions for  $B_c \rightarrow D_s \ell^+ \ell^-$ . (The subscript R represents resonance contribution.)

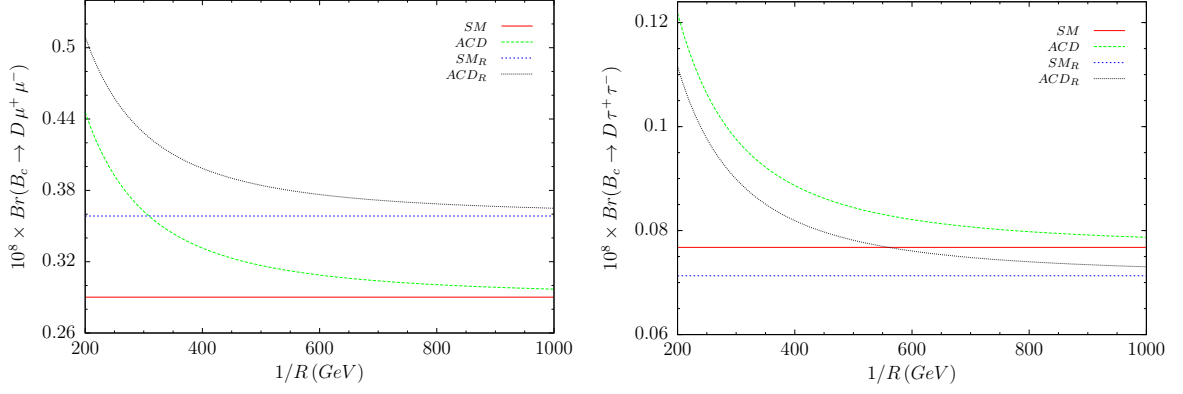


**Figure 6.** (color online) The dependence of branching ratio on  $1/R$  with and without resonance contributions for  $B_c \rightarrow D \ell^+ \ell^-$ .

polarization. Using the convention in [37, 38], we define the orthogonal unit vectors  $S_i^-$  ( $i = L, T, N$ ) for the longitudinal, transverse and normal polarizations in the rest frame of  $\ell^-$  as

$$\begin{aligned}
 S_L^- &\equiv (0, \vec{e}_L) = \left(0, \frac{\vec{p}_\ell}{|\vec{p}_\ell|}\right), \\
 S_T^- &\equiv (0, \vec{e}_T) = (0, \vec{e}_N \times \vec{e}_L), \\
 S_N^- &\equiv (0, \vec{e}_N) = \left(0, \frac{\vec{p}_{D_{q'}} \times \vec{p}_\ell}{|\vec{p}_{D_{q'}} \times \vec{p}_\ell|}\right),
 \end{aligned} \tag{4.1}$$

where  $\vec{p}_\ell$  and  $\vec{p}_{D_{q'}}$  are the three momenta of  $\ell^-$  and  $D_{q'}$  meson in the center of mass (CM) frame of final state leptons, respectively. The longitudinal unit vector  $S_L^-$  is boosted by Lorentz transformation,

$$S_{L,CM}^{-\mu} = \left(\frac{|\vec{p}_\ell|}{m_\ell}, \frac{E_\ell \vec{p}_\ell}{m_\ell |\vec{p}_\ell|}\right), \tag{4.2}$$

while vectors of perpendicular directions remain unchanged under the Lorentz boost.

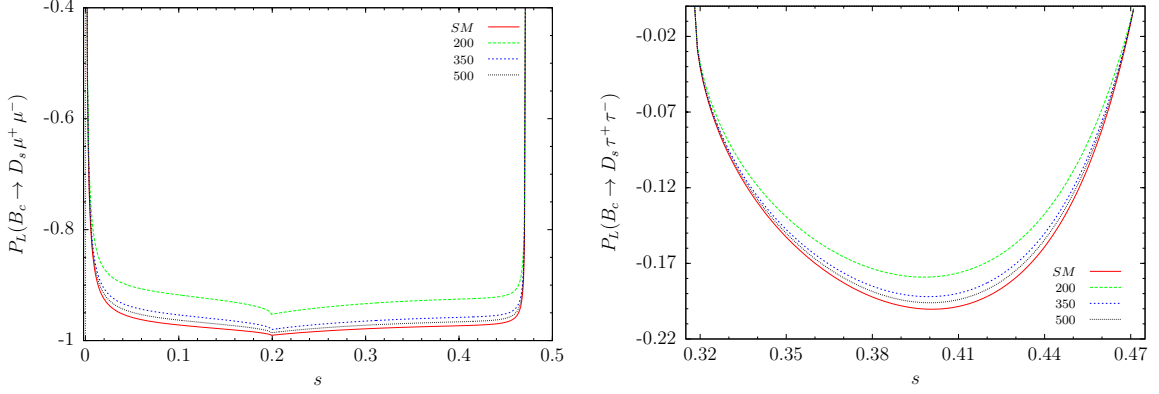


**Figure 7.** (color online) The dependence of longitudinal polarization on  $s$  without resonance contributions for  $B_c \rightarrow D_s \ell^+ \ell^-$ .

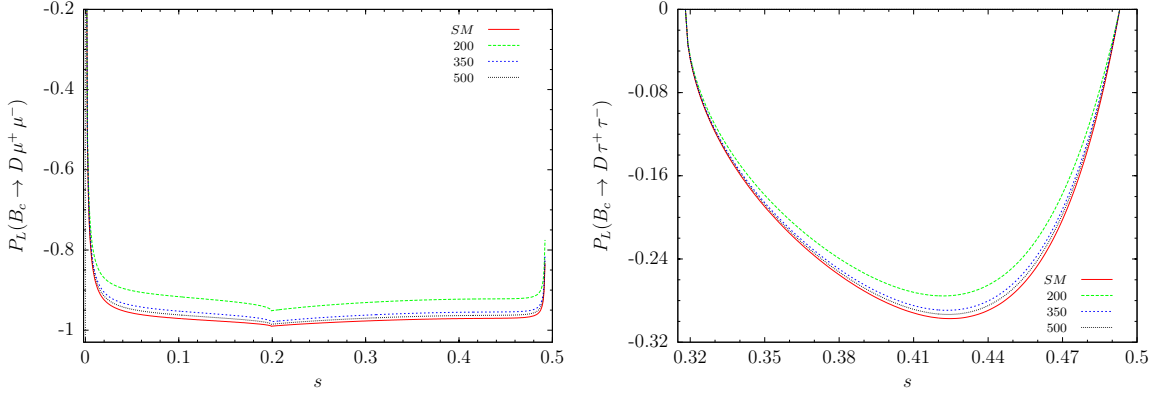


**Figure 8.** (color online) The dependence of longitudinal polarization on  $s$  without resonance contributions for  $B_c \rightarrow D \ell^+ \ell^-$ .

The differential decay rate of  $B_c \rightarrow D_{q'} \ell^+ \ell^-$  for any spin direction  $\vec{n}^-$  of the  $\ell^-$  can be written in the following form

$$\frac{d\Gamma(\vec{n}^-)}{ds} = \frac{1}{2} \left( \frac{d\Gamma}{ds} \right)_0 \left[ 1 + \left( P_L \vec{e}_L^- + P_N^- \vec{e}_N^- + P_T^- \vec{e}_T^- \right) \cdot \vec{n}^- \right], \quad (4.3)$$

where  $(d\Gamma/ds)_0$  corresponds to the unpolarized decay rate, the explicit form of which is given in eq. (3.5).

The polarizations  $P_L^-$ ,  $P_T^-$  and  $P_N^-$  in eq. (4.3) are defined by the equation

$$P_i^-(s) = \frac{d\Gamma(\mathbf{n}^- = \mathbf{e}_i^-)/ds - d\Gamma(\mathbf{n}^- = -\mathbf{e}_i^-)/ds}{d\Gamma(\mathbf{n}^- = \mathbf{e}_i^-)/ds + d\Gamma(\mathbf{n}^- = -\mathbf{e}_i^-)/ds}.$$

Here,  $P_L^-$  and  $P_T^-$  represent the longitudinal and transversal asymmetries, respectively, of the charged lepton  $\ell^-$  in the decay plane, and  $P_N^-$  is the normal component to both of them.



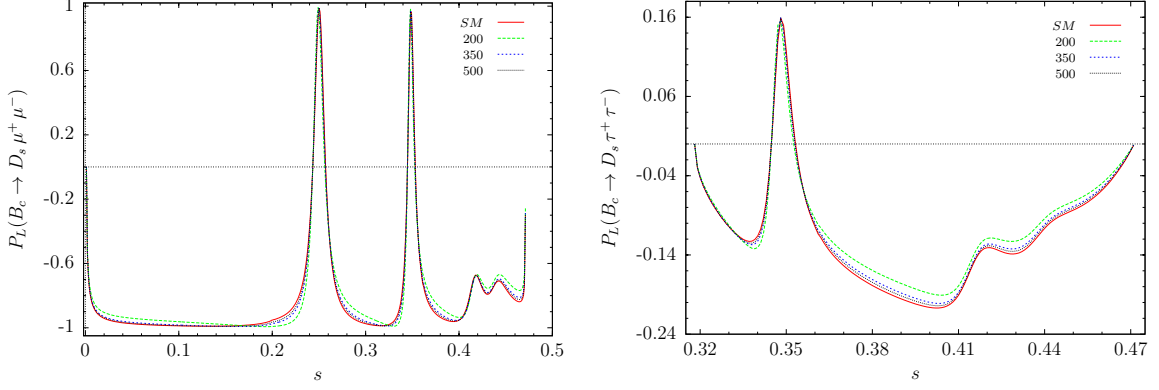


**Figure 9.** (color online) The dependence of longitudinal polarization on  $s$  with resonance contributions for  $B_c \rightarrow D_s \ell^+ \ell^-$ .

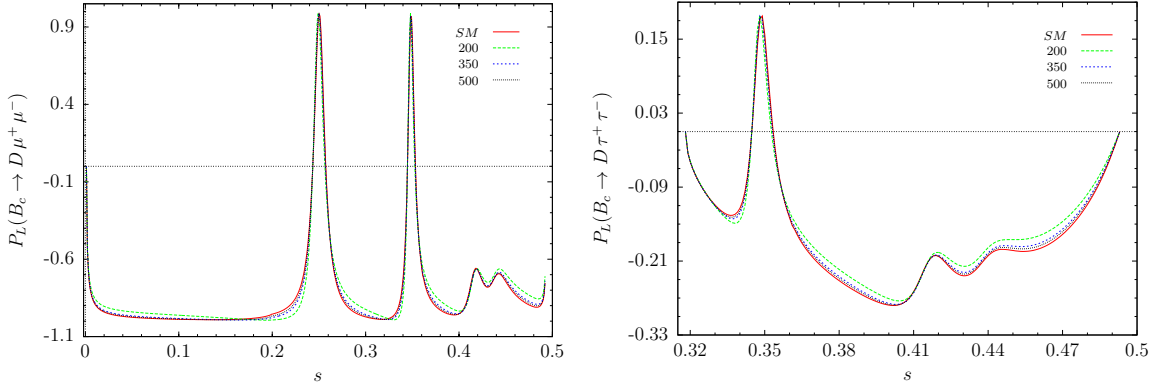


**Figure 10.** (color online) The dependence of longitudinal polarization on  $s$  with resonance contributions for  $B_c \rightarrow D \ell^+ \ell^-$ .

The straightforward calculations yield the explicit form of the longitudinal polarization for  $B_c \rightarrow D_{s,d} \ell^+ \ell^-$  as

$$P_L^- = \frac{16}{3\Delta} m_{B_c}^4 v \lambda \text{Re}[AC^*], \quad (4.4)$$

and the transversal polarization is given by

$$P_T^- = \frac{4m_{B_c}^3 m_\ell \pi \sqrt{s\lambda}}{\Delta} \left[ \frac{(r-1)}{s} \text{Re}[AC^*] + \text{Re}[AD^*] \right]. \quad (4.5)$$

The normal component of polarization is zero so we have not stated its explicit form here.

## 5 Numerical Analysis and Discussion

In this section, we will introduce numerical analysis of physical observables. The input parameters used in this work are  $m_{B_c} = 6.28 \text{ GeV}$ ,  $m_{D_s} = 1.968 \text{ GeV}$ ,  $m_D = 1.870 \text{ GeV}$ ,

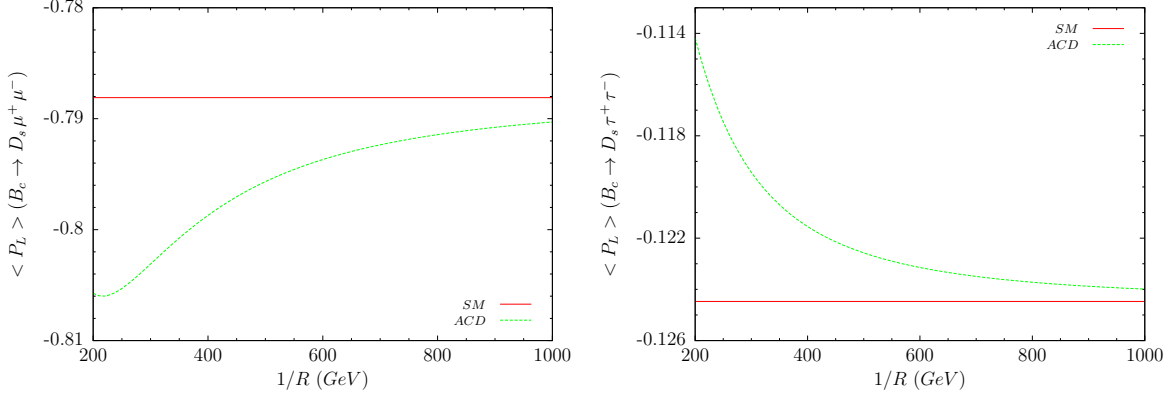


**Figure 11.** (color online) The dependence of longitudinal polarization on  $1/R$  with resonance contributions for  $B_c \rightarrow D_s \ell^+ \ell^-$ .

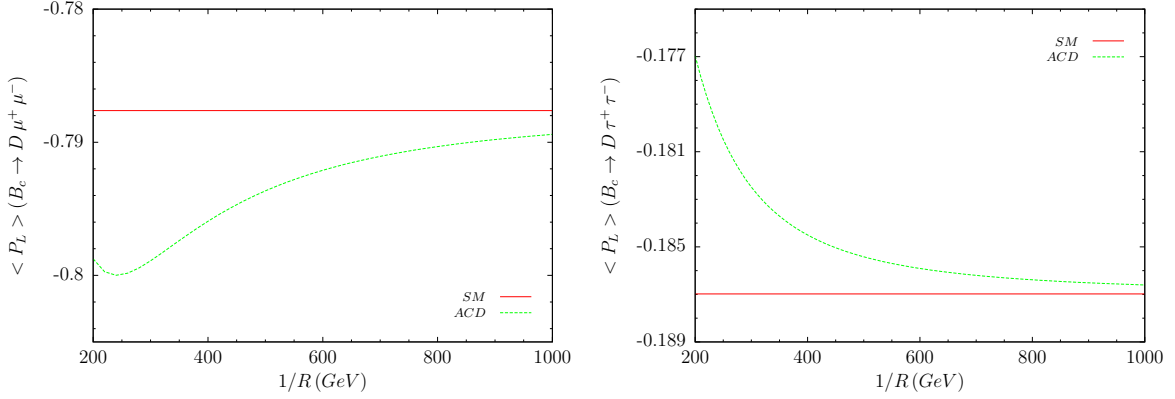


**Figure 12.** (color online) The dependence of longitudinal polarization on  $1/R$  with resonance contributions for  $B_c \rightarrow D \ell^+ \ell^-$ .

$m_b = 4.8 \text{ GeV}$ ,  $m_\mu = 0.105 \text{ GeV}$ ,  $m_\tau = 1.77 \text{ GeV}$ ,  $|V_{tb}V_{ts}^*| = 0.041$ ,  $|V_{tb}V_{td}^*| = 0.008$ ,  $G_F = 1.17 \times 10^{-5} \text{ GeV}^{-2}$  and  $\tau_{B_c} = 0.46 \times 10^{-12} \text{ s}$  [35].

To make numerical predictions, we also need the explicit forms of the form factors  $f_+$ ,  $f_-$  and  $f_T$ . In our analysis, we used the results of [26], calculated in the constituent quark model and  $q^2$  parametrization is given by

$$F(q^2) = \frac{F(0)}{1 - a(q^2/m_{B_c}^2) + b(q^2/m_{B_c}^2)^2},$$

where the values of parameters  $F(0)$ ,  $a$  and  $b$  for the  $B_c \rightarrow (D_s, D)$  decays are listed in Table 1.

In this work, we also took the long-distance contributions into account. While doing this, to minimize the hadronic uncertainties we introduce some cuts around  $J/\psi$  and  $\psi(2s)$  resonances as discussed in [11].

In the analysis, first the differential branching ratios are calculated with and without resonance contributions and  $s$  dependence for  $1/R = 200, 350, 500 \text{ GeV}$  are presented in

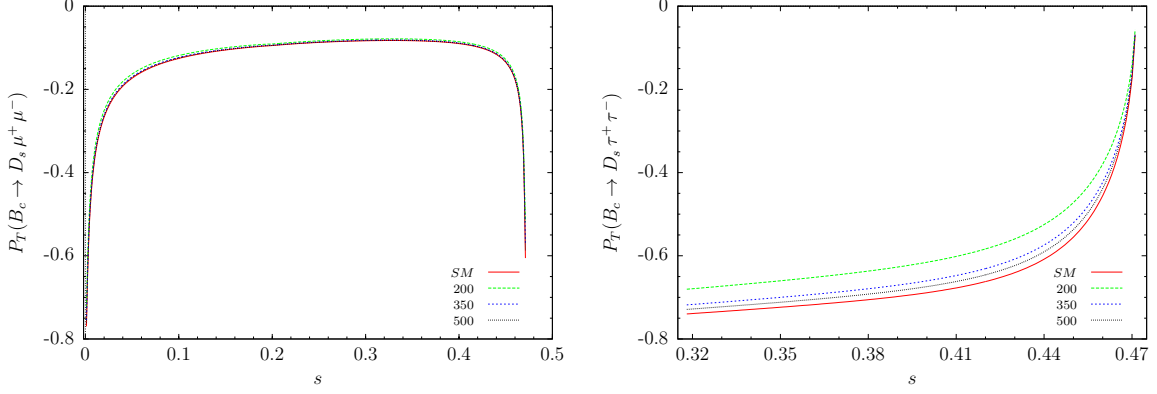


**Figure 13.** (color online) The dependence of transversal polarization on  $s$  without resonance contributions for  $B_c \rightarrow D_s \ell^+ \ell^-$ .

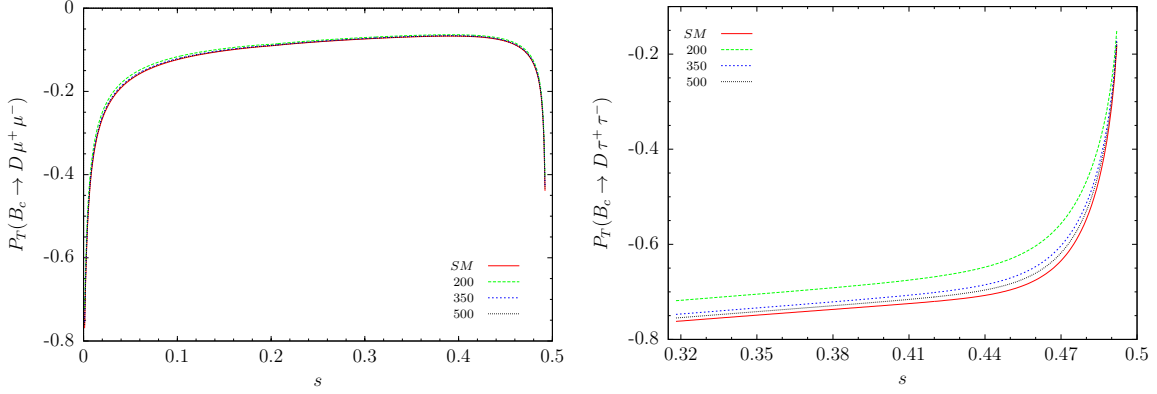


**Figure 14.** (color online) The dependence of transversal polarization on  $s$  without resonance contributions for  $B_c \rightarrow D \ell^+ \ell^-$ .

figures 1–4 for  $B_c \rightarrow (D_s, D) \ell^+ \ell^-$ . One can notice, the change in differential decay rate and difference between the SM results and new effects in the figures. The maximum deviation is around  $s = 0.32$  ( $0.39$ ) in figure 1 and  $s = 0.36$  ( $0.40$ ) in figure 2 for  $\mu(\tau)$ . At these  $s$  values, the deviation is  $\sim 50\%$  more than that of the SM results for  $1/R = 200 \text{ GeV}$  in all decay channels and  $\sim 20\%$  for  $1/R = 350 \text{ GeV}$ . For  $1/R \gtrsim 500 \text{ GeV}$ , the deviation becomes  $\sim 10\%$  and less. Considering the resonance effects, the differential decay rates also differ from their SM values as  $1/R \rightarrow 200 \text{ GeV}$ , which can be seen in figures 3 and 4. So, studying differential decay rate, particularly in  $1/R = 250 - 350 \text{ GeV}$  region, can be an appropriate tool for searching the effect of extra dimension.

To introduce the contributions of the ACD model on the branching ratio, we present  $1/R$  dependent ratios with and without resonance cases in figures 5 and 6. The common feature is that as  $1/R$  increases, the branching ratios approach to their SM values. In all decay channels, for  $1/R \simeq 500 \text{ GeV}$  the deviations are more than  $10\%$  from their SM values. Additionally, around  $1/R \simeq 200 \text{ GeV}$  the ACD contribution is more than  $50\%$ . Keeping the discussion on lower bound on  $1/R$  in mind once again, in the region  $1/R \simeq 350 - 250 \text{ GeV}$  the branching ratios increase with an average of  $(25 - 35)\%$ . So, the calculated branching

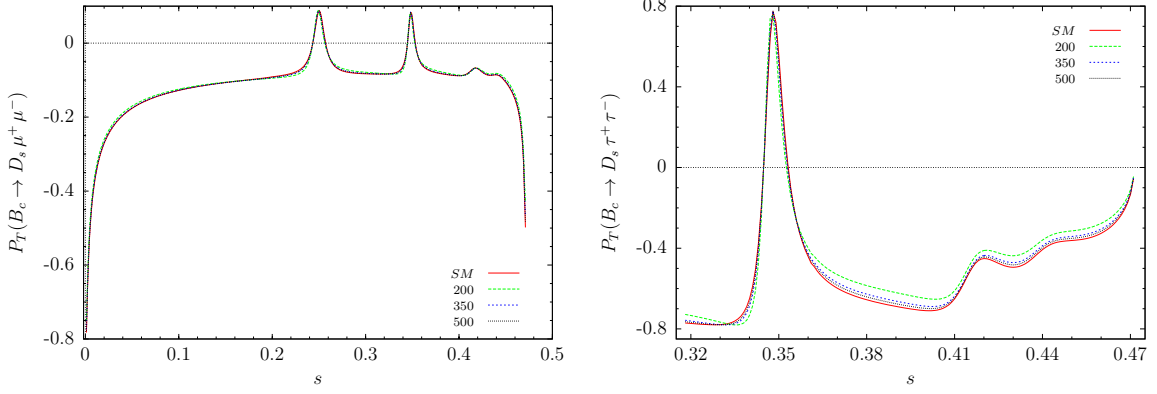


**Figure 15.** (color online) The dependence of transversal polarization on  $s$  with resonance contributions for  $B_c \rightarrow D_s \ell^+ \ell^-$ .

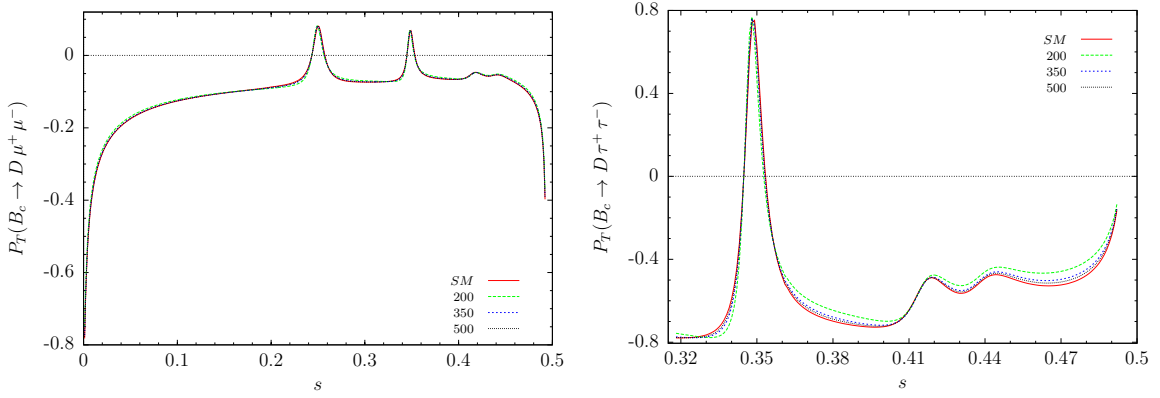


**Figure 16.** (color online) The dependence of transversal polarization on  $s$  with resonance contributions for  $B_c \rightarrow D \ell^+ \ell^-$ .

ratios without resonance contributions for the SM and in between these bounds we find,

$$\begin{aligned}
 Br(B_c \rightarrow D_s \mu^+ \mu^-) &= (1.24, 1.47 - 1.67) \times 10^{-7} \\
 Br(B_c \rightarrow D_s \tau^+ \tau^-) &= (0.29, 0.36 - 0.41) \times 10^{-7} \\
 Br(B_c \rightarrow D \mu^+ \mu^-) &= (0.29, 0.34 - 0.39) \times 10^{-8} \\
 Br(B_c \rightarrow D \tau^+ \tau^-) &= (0.077, 0.092 - 0.106) \times 10^{-8}.
 \end{aligned}$$

Here, the first value in any branching ratios above is corresponding to the SM, while the rests are for  $1/R = 350 - 250 \text{ GeV}$ . A similar behavior is valid for resonance case which can be followed by the figures.

Adding the uncertainty on the form factors may influence the contribution range of the ACD model. However, the variation of the branching ratio, calculated with the central values of form factors, in the ACD model for different  $1/R$ s with the SM values, can be considered as a signal of new physics.

The dependence of longitudinal polarization on  $s$  without resonance contributions are given by figures 7–8. As  $1/R$  approaches to  $200 \text{ GeV}$ , the longitudinal polarization differ

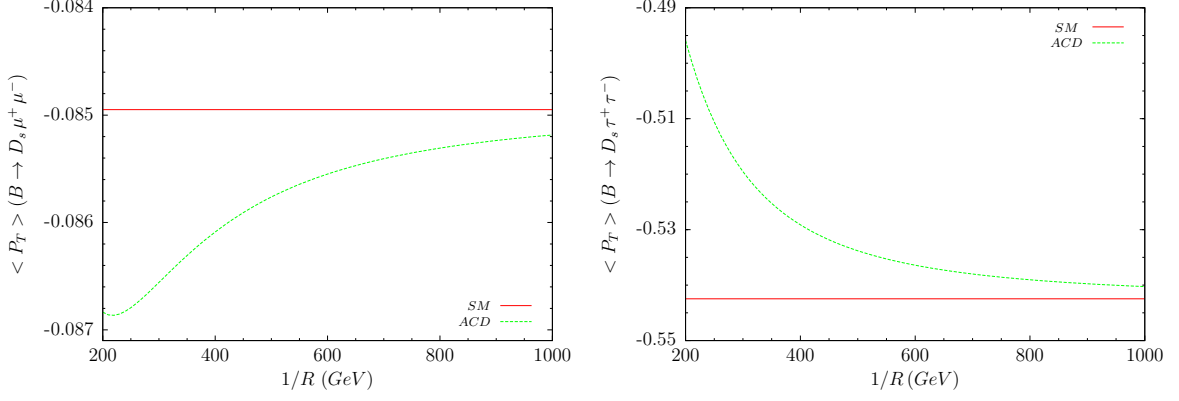


**Figure 17.** (color online) The dependence of transversal polarization on  $1/R$  with resonance contributions for  $B_c \rightarrow D_s \ell^+ \ell^-$ .

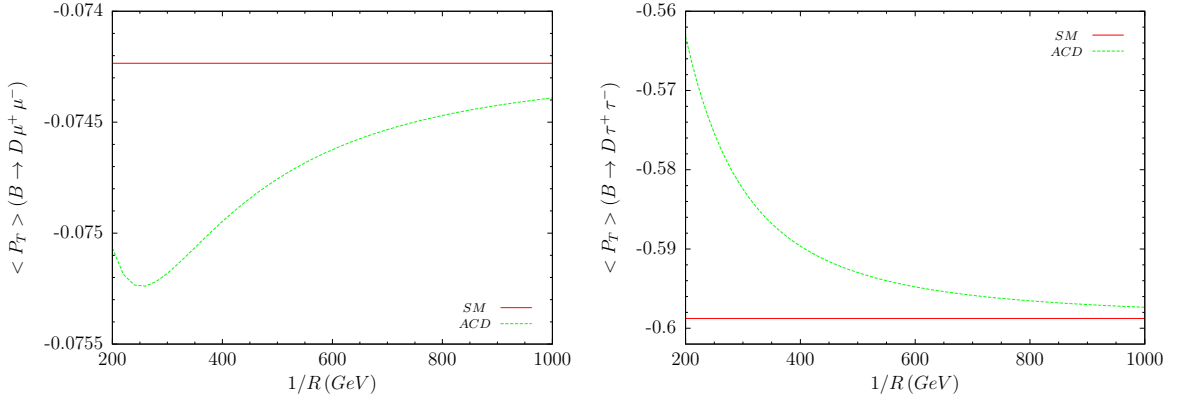


**Figure 18.** (color online) The dependence of transversal polarization on  $1/R$  with resonance contributions for  $B_c \rightarrow D \ell^+ \ell^-$ .

from the SM values, slightly. This is more clear in  $0.34(0.35) \lesssim s \lesssim 0.45(0.47)$  for  $B_c \rightarrow D_s(D)\tau^+\tau^-$  decay, respectively. For  $\mu$  channels, the deviation is valid in all  $s$  range, excluded the minimal and maximal points of  $s$ . In  $B_c \rightarrow D_s(D)\mu^+\mu^-$  decay, the difference is, for example at  $s \sim 0.38$ , 5% (3%), respectively, for  $1/R = 200 \text{ GeV}$ . For  $B_c \rightarrow D_s(D)\tau^+\tau^-$  decay the results are more significant that is at  $s \sim 0.40(0.42)$ , the variation for  $1/R = 200 \text{ GeV}$  is 12% (8%), respectively. Including resonance contributions, in addition to the above effects, deviation between the resonant and nonresonant values increases as  $1/R \rightarrow 200 \text{ GeV}$  (Figures 9 and 10).

In order to clarify the dependence on  $1/R$ , we eliminate the dependence of the lepton polarizations on  $s$ , by considering the averaged forms over the allowed kinematical region as

$$\langle P_i \rangle = \frac{\int_{(2m_\ell/m_{B_c})^2}^{(1-m_{D_{q'}}/m_{B_c})^2} P_i \frac{d\mathcal{B}}{ds} ds}{\int_{(2m_\ell/m_{B_c})^2}^{(1-m_{D_{q'}}/m_{B_c})^2} \frac{d\mathcal{B}}{ds} ds}. \quad (5.1)$$

The  $1/R$  dependant average longitudinal polarizations are given in figures 11 and 12. As

$B_c \rightarrow D_s \ell^+ \ell^-$	$F(0)$	$a$	$b$
$f_+$	0.165	-3.40	3.21
$f_-$	-0.186	-3.51	3.38
$f_T$	-0.258	-3.41	3.30
$B_c \rightarrow D \ell^+ \ell^-$	$F(0)$	$a$	$b$
$f_+$	0.126	-3.35	3.03
$f_-$	-0.141	-3.63	3.55
$f_T$	-0.199	-3.52	3.38

**Table 1.**  $B_c \rightarrow D_{s,d}$  decays form factors calculated in the constitute quark model.

it can be seen from the figures, the maximum deviation is 2% for  $\mu$  channels and 9% (6%) for  $B_c \rightarrow D_s(D)\tau^+\tau^-$ , respectively, at  $1/R = 200 \text{ GeV}$ .

The variation of transversal polarization with respect to  $s$  are given by figures 13-16. In  $\mu$  channels the difference is negligible whereas in  $\tau$  channels up to  $s \sim 0.46$  (0.48) for  $B_c \rightarrow D_s(D)\ell^+\ell^-$  decays, respectively, the effects of the UED can be seen. At, for example,  $s \sim 0.40$  (0.44), the SM value vary 5 – 12% (4 – 9%) for  $1/R = 350 - 200 \text{ GeV}$ , respectively. Finally, the average transversal polarization can be followed by figures 17 and 18. For the  $\mu$  channels the maximum deviation is 2% and for  $B_c \rightarrow D_s(D)\tau^+\tau^-$  that is 10%(6%) at  $1/R = 200 \text{ GeV}$ .

As an overall conclusion, as  $1/R \rightarrow 200 \text{ GeV}$  the physical values differ from the SM results. Up to a few hundreds GeV above  $250 \text{ GeV}$  or  $350 \text{ GeV}$ , which are more common lower bounds, one can see the effects of UED. Considering the differential and integrated branching ratios, there appears essential difference, particularly in between  $1/R = 250 - 350 \text{ GeV}$  comparing with the SM results. The polarization effects in  $\mu$  channels are either irrelevant nor negligible while in  $\tau$  channels small effects are obtained. Under the discussion in this work, studying these decays experimentally can be useful.

## References

- [1] I. Antoniadis, Phys. Lett. B **246** (1990) 377.
- [2] I. Antoniadis, N. Arkani-Hamed, S. Dimopoulos and G. Dvali, Phys. Lett. B **436** (1998) 257, arXiv:hep-ph/9804398.
- [3] N. Arkani-Hamed, S. Dimopoulos and G. Dvali, Phys. Lett. B **429** (1998) 263, arXiv:hep-ph/9803315.
- [4] N. Arkani-Hamed, S. Dimopoulos and G. Dvali, Phys. Rev. D **59** (1999) 086004, arXiv:hep-ph/9807344
- [5] T. Appelquist, H. C. Cheng and B. A. Dobrescu, Phys. Rev. D **64** (2001) 035002, arXiv:hep-ph/0012100.
- [6] K. Agashe, N. G. Deshpande and G. H. Wu, Phys. Lett. B **511** (2001) 85 , **B514**, 309 (2001), arXiv:hep-ph/0103235.
- [7] P. Colangelo, F. De Fazio, R. Ferrandes and T. N. Pham, Phys. Rev. D **73** (2006) 115006, arXiv:0709.2817 [hep-ph].
- [8] U. Haisch and A. Weiler, Phys. Rev D **76** (2007) 034014, arXiv:hep-ph/0703064.
- [9] P. Biancofiore, P. Colangelo and F. Fazio, Phys. Rev. D **85** (2012) 094012, arXiv:1202.2289 [hep-ph].
- [10] K. Azizi, *et. al.*, JHEP **1205** (2012) 024, arXiv:1203.4356[hep-ph].
- [11] U. O. Yilmaz, Phys. Rev. D **85** (2012) 115026, arXiv:1204.1261 [hep-ph].
- [12] A. J. Buras, M. Spranger and A. Weiler, Nucl. Phys. B **660**, 225 (2003), arXiv:hep-ph/0212143.
- [13] A. J. Buras, A. Poschenrieder, M. Spranger and A. Weiler, Nucl. Phys. B **678**, 455 (2004) arXiv:hep-ph/0306158.
- [14] P. Colangelo, F. De Fazio, R. Ferrandes and T. N. Pham, Phys. Rev. D **74** (2006) 115006, arXiv:hep-ph/0610044.
- [15] G. Devidze, A. Liparteliani and U. G. Meissner, Phys. Lett. B **634** (2006) 59, arXiv:hep-ph/0510022.
- [16] R. Mohanta and A. K. Giri, Phys. Rev. D **75** (2007) 035008, arXiv:hep-ph/0611068.
- [17] P. Colangelo, F. De Fazio, R. Ferrandes and T. N. Pham, Phys. Rev. D **77** (2008) 055019, arXiv:hep-ph/0604029.
- [18] A. Saddique, M. J. Aslam and C. D. Lu, Eur. Phys. J. C **56** (2008) 267, arXiv:0803.0192 [hep-ph].
- [19] I. Ahmed, M. A. Paracha and M. J. Aslam, Eur. Phys. J. C **54** (2008) 591, arXiv:0802.0740 [hep-ph].
- [20] V. Bashiry and K. Zeynali, Phys. Rev. D **79** (2009) 033006, arXiv:0805.3386 [hep-ph].
- [21] M. V. Carlucci, P. Colangelo and F. De Fazio, Phys. Rev. D **80** (2009) 055023, arXiv:0907.2160 [hep-ph].
- [22] Y. Li and J. Hua, Eur. Phys. J. C **71** (2011) 1764, arXiv:1105.3031 [hep-ph].
- [23] T. M. Aliev and M. Savci, Eur. Phys. J. C **50** (2007) 91, arXiv:hep-ph/0606225.

- [24] N. Katirci and K. Azizi, JHEP **1101** (2011) 087, arXiv:1011.5647 [hep-ph].
- [25] N. Katirci and K. Azizi, JHEP **1107** (2011) 043, arXiv:1105.3636 [hep-ph].
- [26] C. Q. Geng, C. W. Hwang and C. C. Liu, Phys. Rev. D **65** (2002) 094037, arXiv:hep-ph/0110376.
- [27] A. Faessler, Th. Gutsche, M. A. Ivanov, J. G. Körner and V. E. Lyubovitskij, Eur. Phys. J. direct C **4** (2002) 18, arXiv:hep-ph/0205287.
- [28] H.-M. Choi, Phys. Rev. D **81** (2010) 054003, arXiv:1001.3432 [hep-ph].
- [29] D. Ebert, R. N. Faustov and V. O. Galkin, Phys. Rev. D **82** (2010) 034032, arXiv:1006.4231 [hep-ph].
- [30] K. Azizi and R. Khosravi, Phys. Rev. D **78** (2008) 036005, arXiv:0806.0590 [hep-ph].
- [31] G. Buchalla, A. J. Buras and M. Lautenbacher, Rev. Mod. Phys. **68** (1996) 1125, arXiv:hep-ph/9512380.
- [32] A. J. Buras and M. Münz, Phys. Rev. D **52**, (1995)186, arXiv:hep-ph/9501281.
- [33] M. Misiak, Nucl. Phys. **B 393**, (1993) 23, **B 439**, (1995) 461(E).
- [34] A. Ali, T. Mannel and T. Morozumi, Phys. Lett. B **273**, (1991) 505 .
- [35] K. Nakamura, *et al.* (Particle Data Group), J. Phys. G **37**, (2010) 075021 .
- [36] A. Ali, P. Ball, L. T. Handoko and G. Hiller, Phys. Rev. D **61**, (2000) 074024, arXiv:hep-ph/9910221.
- [37] S. Fukae, C. S. Kim and T. Yoshikawa, Phys. Rev. D **61**, (2000) 074015, arXiv:hep-ph/9908229.
- [38] F. Krüger and L. M. Sehgal, Phys. Lett. B **380**, 199 (1996), arXiv:hep-ph/9603237.